

---

# PERSONALIZED FEDERATED LEARNING: AN ATTENTIVE COLLABORATION APPROACH

---

A PREPRINT

**Yutao Huang**  
Simon Fraser University  
Burnaby, Canada  
yutaoh@sfu.ca

**Lingyang Chu**  
Huawei Technologies Canada  
Burnaby, Canada  
lingyang.chu1@huawei.com

**Zirui Zhou**  
Huawei Technologies Canada  
Burnaby, Canada  
zirui.zhou@huawei.com

**Lanjun Wang**  
Huawei Technologies Canada  
Burnaby, Canada  
lanjun.wang@huawei.com

**Jiangchuan Liu**  
Simon Fraser University  
Burnaby, Canada  
jcliu@sfu.ca

**Jian Pei**  
Simon Fraser University  
Burnaby, Canada  
jpei@cs.sfu.ca

**Yong Zhang**  
Huawei Technologies Canada  
Burnaby, Canada  
yong.zhang3@huawei.com

July 9, 2020

## ABSTRACT

For the challenging computational environment of IOT/edge computing, personalized federated learning allows every client to train a strong personalized cloud model by effectively collaborating with the other clients in a privacy-preserving manner. The performance of personalized federated learning is largely determined by the effectiveness of inter-client collaboration. However, when the data is non-IID across all clients, it is challenging to infer the collaboration relationships between clients without knowing their data distributions. In this paper, we propose to tackle this problem by a novel framework named federated attentive message passing (FEDAMP) that allows each client to collaboratively train its own personalized cloud model without using a global model. FEDAMP implements an attentive collaboration mechanism by iteratively encouraging clients with more similar model parameters to have stronger collaborations. This adaptively discovers the underlying collaboration relationships between clients, which significantly boosts effectiveness of collaboration and leads to the outstanding performance of FEDAMP. We establish the convergence of FEDAMP for both convex and non-convex models, and further propose a heuristic method that resembles the FEDAMP framework to further improve its performance for federated learning with deep neural networks. Extensive experiments demonstrate the superior performance of our methods in handling non-IID data, dirty data and dropped clients.

## 1 Introduction

Huge amount of edge devices (i.e., clients), such as smart phones, wearable devices and autonomous vehicles, are generating big private data in a surprisingly fast speed [1]. Due to the ever-growing concerns and restrictions on data privacy, many federated learning frameworks have been proposed to collaboratively conduct machine learning tasks for all clients while keeping their data privacy intact [2, 3, 4, 5, 6, 7].

One of the biggest challenges for federated learning is **non-IID data**, that is, the data is non-IID across different clients [3, 4, 8]. Since it is difficult for a single model to properly fit the non-IID data of all clients [8], existing federated learning frameworks that focus on training a single global model cannot achieve a good personalized performance

on each of the clients. As a result, it is more reasonable to conduct **personalized federated learning**, such that every client can train a strong personalized model without leaking its private data by effectively collaborating with the other clients in a federated manner.

The performance of personalized federated learning is largely determined by the **effectiveness of inter-client collaboration**, which, however, is a challenging goal to optimize when the private data held by the clients is non-IID. Since the data distributions of two clients can either be similar or different, an effective inter-client collaboration should allow closely related clients with similar data distributions to have stronger collaboration than those with different data distributions. However, as illustrated later in Sec. 2, most existing methods [9, 10, 11, 12, 13, 14, 15, 16] that produce personalized models by locally customizing a global model cannot effectively identify the underlying collaboration relationships between clients. This reduces the effectiveness of inter-client collaboration and largely limits the performance of personalized models.

In this paper, we tackle the challenging personalized federated learning problem by an **attentive collaboration mechanism** that adaptively discovers the underlying inter-client collaboration relationships to achieve outstanding personalized performance without using a global model. We make the following contributions. **First**, we propose a novel method named federated attentive message passing (FEDAMP) to realize the attentive collaboration mechanism. FEDAMP adopts an attention-inducing function to bind a **personalized cloud model** with each client’s **local model**. In this way, the attentive collaboration can be easily conducted by iteratively passing strong model aggregation messages between similar local models and personalized cloud models. This discovers the underlying collaboration relationships between clients, and further boosts their collaboration effectiveness. **Second**, we prove the convergence of FEDAMP for both convex and non-convex models. **Third**, to further improve the practical performance of FEDAMP on clients using deep neural networks, we propose a heuristic method to avoid the scaling problem of high dimensional model parameters of clients by measuring their model similarity with cosine similarity. **Last**, we conduct extensive experiments to demonstrate the superior performance of the proposed methods in challenging federated learning settings, such as non-IID data, dropped clients and dirty data.

## 2 Related Works

**Global federated learning.** The goal of global federated learning is to learn a single global model that minimizes the empirical risk function over the union of the data across all clients. FedAvg [2] trains local models of clients in parallel and produces a global model by simply averaging the parameters of local models. However, it has been empirically shown to diverge on non-IID data across clients [2, 3, 4]. To improve the robustness of FedAvg to non-IID data, FedProx [3] adds a proximal term to keep local models close to the global model, and Zhao et al. [4] globally share a small subset of data across all clients. For clients using deep neural networks, FedAtt [17] aggregates local models into a global model by a layer-wise attention mechanism, PFNM [18] addresses the invariance problem of fully connected feedforward networks by matching the neurons of client neural networks before averaging them, and FedMA [19] further extends PFNM to more complicated deep neural networks by exploring the layers-wise invariance of CNNs and LSTMs. Most global federated learning methods use a single global model for all clients. However, when the data is non-IID across different clients, it will be difficult to converge to a good global model that achieves a good personalized performance on each of the clients [8].

**Local customization of a global model.** The most practical way to build a personalized model for a client is to customize a global model by local fine-tuning [10, 11, 12, 20, 21, 22], where the parameters of the global model are used as the initialization to train a personalized model on the local data of every client. Similarly, some meta learning methods [9, 15, 16, 23, 24, 25] can be extended to build personalized models by adapting a trained global model on the local data of a client with a few fine-tuning steps [8]. Besides, model mixture methods [13, 14] are also proposed to locally customize a global model for each client by linearly combining the global model and the client’s latent local model. All these methods require a good global model for local customization. However, since the private data distributions of the clients are unknown, the global model is usually trained by taking equal or weighted contributions from all clients without considering their underlying collaboration relationships. This inevitably reduces the effectiveness of inter-client collaboration, and further degenerates the performance of personalized models when the data is non-IID.

**Multi-Task Learning.** Multi-task learning aims to train personalized models for multiple related tasks in a centralized manner by either assuming the structure of the relationships between tasks to be known apriori [26, 27, 28, 29], or attempting to learn the relationships between tasks from data [30, 31, 32]. These methods focus on learning personalized models for different tasks, but ignore the data privacy of clients. Therefore, they are not applicable to federated learning. Distributed multi-task learning [33, 34, 35, 36] tried to conduct multi-task learning when the data for each task is separately owned by different clients. While these methods have the potential to protect the data privacy of clients, they cannot robustly handle the unreliable operating environment of federated learning [37]. To tackle these challenges,

Smith et al. [37] extend distributed multi-task learning to federated learning by a primal-dual optimization method, which, however, is not applicable to deep neural networks because strong duality is no longer guaranteed.

### 3 Personalized Federated Learning

In this section, we illustrate how to tackle the **personalized federated learning problem**, where a set of clients, each owning a personalized model and a set of private data collected from distinct distributions, attempt to train their personalized models by effectively collaborating with each other in a privacy-preserving manner under the coordination of a service provider [4, 8]. We first introduce how to tackle this problem by a general framework named FEDAMP in Sec. 3.1, then we discuss a specific instantiation of FEDAMP as well as a practical heuristic extension called HEURFEDAMP in Sec. 3.2 and Sec. 3.3, respectively. Last, we prove the convergence of FEDAMP for both convex and non-convex local models in Sec. 3.4.

#### 3.1 Federated Attentive Message Passing

Federated attentive message passing (FEDAMP) is a general framework to tackle the personalized federated learning problem. The **key idea** is to iteratively encourage clients with similar model parameters to have much stronger collaboration than clients with dissimilar ones, such that, we can adaptively discover the underlying collaboration relationships between clients, and further boosts their collaboration effectiveness. Specifically, FEDAMP promotes effective inter-client collaboration by realizing an **attentive collaboration mechanism** that iteratively encourages clients with more similar model parameters to have stronger collaborations.

For a personalized federated learning system of  $m$  clients, we denote by  $w_i \in \mathbb{R}^d$ ,  $i \in \{1, \dots, m\}$ , the parameters of the **local model** of the  $i$ -th client, and by  $F_i : \mathbb{R}^d \rightarrow \mathbb{R}$  the training objective function of the  $i$ -th client. We will illustrate how to derive the **personalized cloud model** for each client later in this subsection. Inspired by several widely adopted formulations in multi-task learning [38, 39], we formulate the personalized federated learning problem as

$$\min_{w_1, \dots, w_m} \left\{ \mathcal{G}(w_1, \dots, w_m) := \sum_{i=1}^m F_i(w_i) + \lambda \cdot \sum_{i < j}^m D(w_i, w_j) \right\}, \quad (1)$$

where the first term is the training loss of the local models of all clients,  $\lambda > 0$  is a regularization parameter, and  $D(\cdot, \cdot)$  is a regularization function to measure the difference between its inputs. Here, the formulation in (1) is a general form that represents a class of objective functions for different user-specified functions  $D$ . The second term of (1) will enforce the attentive collaboration mechanism if  $D$  is properly chosen to be an **attention-inducing function** defined as follows.

**Definition 1** We say that  $D$  is an attention-inducing function if  $D(x, y) = \mathcal{A}(\|x - y\|^2)$  for some nonlinear function  $\mathcal{A} : [0, \infty) \rightarrow \mathbb{R}$  satisfying

- (i)  $\mathcal{A}$  is increasing and concave on  $[0, \infty)$  with  $\mathcal{A}(0) = 0$ ;
- (ii)  $\mathcal{A}$  is continuously differentiable on  $(0, \infty)$  and  $\lim_{t \rightarrow 0^+} \mathcal{A}'(t) = a$  for some  $a < \infty$ .

As illustrated later in this subsection, the attention-inducing function  $D$  is the key to inducing the attentive collaboration mechanism.

We propose to tackle the problem formulated in (1) by a novel algorithm named FEDAMP, which is powered by an incremental-type optimization method ([40]) and is carefully deployed on the client-sever system to fit the privacy-preserving requirement of personalized federated learning.

Specifically, FEDAMP optimizes the  $\mathcal{G}(w_1, \dots, w_m)$  in (1) by alternatively optimizing its two components, denoted by  $\mathcal{F}(W) := \sum_{i=1}^m F_i(w_i)$  and  $\mathcal{D}(W) := \sum_{i < j}^m D(w_i, w_j)$ , where  $W = [w_1, \dots, w_m]$  is a  $d$ -by- $m$  dimensional matrix whose columns  $(w_1, \dots, w_m)$  are the model parameters for the **local models** of the clients  $(1, \dots, m)$ , respectively.

Denote by  $W^{k-1} = [w_1^k, \dots, w_m^k]$  the iterate in the  $k$ -th iteration, we first apply a gradient descent step to  $\mathcal{D}$  to compute an intermediate variable

$$U^k = W^{k-1} - \alpha_k \nabla \mathcal{D}(W^{k-1}), \quad (2)$$

where  $\alpha_k > 0$  is the step size, and  $U^k = [u_1^k, \dots, u_m^k]$  is a  $d$ -by- $m$  dimensional matrix whose columns  $(u_1^k, \dots, u_m^k)$  are the model parameters for the **personalized cloud models** of the clients  $(1, \dots, m)$ , respectively. Then, we use  $U^k$  as the prox-center and apply a proximal point step [41] to compute the next iterate

$$W^k = \arg \min_W \mathcal{F}(W) + \frac{\lambda}{2\alpha_k} \|W - U^k\|^2. \quad (3)$$

**Algorithm 1:** Federated Attentive Message Passing (FEDAMP)

---

**Input:** The number of clients  $m$ , initial models  $(w_1^0, \dots, w_m^0)$ , total communication rounds  $K$ , gradient descent step sizes  $\{\alpha_k\}$ , parameters  $\{\beta_k\}$  for local training

- 1 **for**  $k = 1, 2, \dots, K$  **do**
- 2     Server computes the personalized cloud models  $(u_1^k, \dots, u_m^k)$  by (4)
- 3     Server sends each  $u_i^k$  to client  $i$
- 4     Clients perform local training and update the models  $(w_1^k, \dots, w_m^k)$  by (5)
- 5     Server collects the updated models  $(w_1^k, \dots, w_m^k)$
- 6 **end**

---

This procedure terminates at some iteration  $K$  that is prescribed as the maximum number of iterations. We provide the non-asymptotic convergence guarantee of this optimization algorithm in Sec. 3.4.

Algorithm 1 summarizes how FEDAMP deploys the above optimization method on a client-server platform to conduct personalized federated learning.

**First**, the iteration of FEDAMP starts with an initial guess of the model parameters, denoted by  $(w_1^0, \dots, w_m^0)$ . These parameters are first obtained by separately pre-training the personalized models of each client using their local data, and then collected and stored on the server.

**Second**, at the  $k$ -th communication round, the server computes a set of personalized cloud models  $(u_1^k, \dots, u_m^k)$  by (2). Since  $\mathcal{D}(W) = \sum_{i < j}^m D(w_i, w_j)$  and the function  $D$  is an attention-inducing function in Definition 1, (2) can be equivalently written as

$$u_i^k = \left( 1 - \alpha_k \sum_{j \neq i}^m \mathcal{A}'(\|w_i^{k-1} - w_j^{k-1}\|^2) \right) \cdot w_i^{k-1} + \alpha_k \sum_{j \neq i}^m \mathcal{A}'(\|w_i^{k-1} - w_j^{k-1}\|^2) \cdot w_j^{k-1} \quad (4)$$

for all  $i \in \{1, \dots, m\}$ , where  $u_i^k$  is simply a weighted average of  $(w_1^{k-1}, \dots, w_m^{k-1})$ .

**Third**, the server sends each personalized cloud model  $u_i^k$  to client  $i$  and requests it to perform local training with the knowledge of  $u_i^k$ . Following (3), client  $i$  computes an updated local model  $w_i^k$  by

$$w_i^k = \arg \min_{w \in \mathbb{R}^d} F_i(w) + \frac{1}{2\beta_k} \|w - u_i^k\|^2 \quad (5)$$

with  $\beta_k = \alpha_k/\lambda$ , where  $\lambda$  is the regularization parameter in (1).

**Last**, the server collects the updated local models  $(w_1^k, \dots, w_m^k)$  and the system enters the  $(k+1)$ -th communication round. When FEDAMP terminates at the  $K$ -th round for some user-specified  $K$ , each client  $i$  holds a pair of  $u_i^K$  and  $w_i^K$ , which can both be used for personalied inference tasks.

Now we discuss why FEDAMP can be viewed as a message passing approach that realizes the attentive collaboration mechanism without infringing the data privacy of all clients.

**First of all**, since FEDAMP never transfers the private data of any client, the data privacy of all clients is kept intact during the entire training process.

**Second**, FEDAMP is a message passing approach. We can observe from (4) that the cloud model  $u_i^k$  can be rewritten in the following form

$$u_i^k = \xi_{i,1} w_1^{k-1} + \dots + \xi_{i,m} w_m^{k-1} \quad (6)$$

where  $\xi_{i,1} + \dots + \xi_{i,m} = 1$ , and  $(\xi_{i,1}, \dots, \xi_{i,m})$  are linear combination weights for the client model parameters  $(w_1^{k-1}, \dots, w_m^{k-1})$ . Obviously, the client model parameters  $(w_1^{k-1}, \dots, w_m^{k-1})$  can be viewed as the **messages** that are **passed** from all clients to the  $i$ -th client, and the model parameters  $u_i^k$  of client  $i$ 's personalized cloud model is a weighted aggregation of the messages received from all clients. As a result, FEDAMP is a message passing approach that conducts inter-client collaboration by passing messages between local models and personalized cloud models.

**Last**, FEDAMP realizes the attentive collaboration mechanism. To see this, we rewrite (4) as

$$u_i^k = \tau_{k,i} w_i^{k-1} + (1 - \tau_{k,i}) z_i^{k-1}, \quad (7)$$

where

$$z_i^{k-1} = \frac{\sum_{j \neq i}^m \mathcal{A}'(\|w_i^{k-1} - w_j^{k-1}\|^2) \cdot w_j^{k-1}}{\sum_{j \neq i}^m \mathcal{A}'(\|w_i^{k-1} - w_j^{k-1}\|^2)}, \quad (8)$$

---

**Algorithm 2:** A Heuristic Extension of FEDAMP (HEURFEDAMP)

---

**Input:** The number of clients  $m$ , initial models  $(w_1^0, \dots, w_m^0)$ , total communication rounds  $K$ , self-attention parameters  $\{\tau_{k,i}\}$ , parameters  $\{\beta_{k,i}\}$  for local training

1 **for**  $k = 1, 2, \dots, K$  **do**

2     For every  $i = 1, \dots, m$ , server computes the attentive aggregation of  $\{w_j^{k-1}\}_{j \neq i}$  by

$$z_i^{k-1} = \frac{\sum_{j \neq i}^m e^{\sigma \cos(w_i^{k-1}, w_j^{k-1})} \cdot w_j^{k-1}}{\sum_{j \neq i}^m e^{\sigma \cos(w_i^{k-1}, w_j^{k-1})}}. \quad (10)$$

3     For every  $i = 1, \dots, m$ , server computes the personalized cloud model  $u_i^k$  by

$$u_i^k = (1 - \tau_{k,i})w_i^{k-1} + \tau_{k,i}z_i^{k-1} \quad (11)$$

5     Server sends each  $u_i^k$  to client  $i$

6     Every client  $i$  computes an updated local models  $w_i^k$  by (5) with  $\beta_{k,i}$

7     Server collects the updated local models  $(w_1^k, \dots, w_m^k)$

8 **end**

---

is an aggregation of the messages from all the clients other than client  $i$ , and  $\tau_{k,i} = 1 - \alpha_k \sum_{j \neq i}^m \mathcal{A}'(\|w_i^{k-1} - w_j^{k-1}\|^2)$  is a scalar self-attention parameter that balances the contribution of the messages received by  $w_i^k$  from client  $i$  and the other clients. Recall Definition 1 that  $\mathcal{A}$  is increasing and concave on  $[0, \infty)$ , which implies that its derivative  $\mathcal{A}'$  is non-negative and non-increasing on  $(0, \infty)$ . Thus, the  $z_i^{k-1}$  in (8) is a convex combination of  $\{w_j^{k-1} : j \neq i\}$ . Since the weight of each  $w_j^{k-1}$  in (8) is non-negative and its magnitude is a non-increasing function of the Euclidean distance between  $w_j^{k-1}$  and  $w_i^{k-1}$ , a  $w_j^{k-1}$  that is similar to  $w_i^{k-1}$  contributes more to the aggregation (8). In this way, FEDAMP iteratively encourages clients with more similar model parameters to have stronger collaborations. As a result, FEDAMP realizes the attentive collaboration mechanism.

It is worth mentioning that the mechanism of collaboration in FEDAMP is blind to the clients. This means each client receives a tailored cloud model  $u_i^k$  without knowing the collaboration graph, which further improves the privacy of all clients during training.

### 3.2 An Instance of FEDAMP

The FEDAMP proposed in Algorithm 1 needs to be instantiated by specifying the attention-inducing function. The class of attention-inducing functions is broad. In particular, examples of function  $\mathcal{A}$  that satisfies the conditions (i) and (ii) in Definition 1 includes the negative exponential function  $\mathcal{A}(t) = 1 - e^{-t/\sigma}$  and the tamed square root function  $\mathcal{A}(t) = t/(2\sigma)$  if  $t \in [0, \sigma^2]$  and  $\mathcal{A}(t) = \sqrt{t} - \sigma/2$  if  $t > \sigma^2$ , where  $\sigma > 0$  is a parameter that can be chosen by the user. Also, the smoothly clipped absolute deviation (SCAD) function [42] and the minimax concave penalty (MCP) function [43], which are popular for inducing sparse estimators in high-dimensional statistics, are also examples that satisfy (i) and (ii).

Next, we use the negative exponential function  $\mathcal{A}(t) = 1 - e^{-t/\sigma}$  as an example to further illustrate the attention mechanism in FEDAMP. With  $\mathcal{A}(t) = 1 - e^{-t/\sigma}$ , the  $z_i^{k-1}$  in (8) can be written as

$$z_i^{k-1} = \frac{\sum_{j \neq i}^m e^{-\frac{\|w_i^{k-1} - w_j^{k-1}\|^2}{2\sigma}} \cdot w_j^{k-1}}{\sum_{j \neq i}^m e^{-\frac{\|w_i^{k-1} - w_j^{k-1}\|^2}{2\sigma}}}, \quad (9)$$

which is then used to construct the personalized cloud model  $u_i^k$  via (7). Note that  $K(x, y) = e^{-\|x-y\|^2/2\sigma}$  is the so-called radial basis function (RBF) kernel that is broadly used in kernelized learning algorithms as a similarity measure [44]. Then, from (7) and (9), we can observe that for every  $j \neq i$ , the contribution of  $w_j^{k-1}$  to the personalized cloud model  $u_i^k$  for client  $i$  is proportional to the similarity between  $w_i^{k-1}$  and  $w_j^{k-1}$ , where the similarity is measured by the RBF kernel. This induces an attentive mechanism of collaboration as desired.

### 3.3 A Heuristic Extension of FEDAMP

Recall from (7) and (8) that in the attentive mechanism of FEDAMP, the similarity between any two models is measured as a function of their Euclidean distance; see (9) for an example. However, this may be inadequate for application domains where the Euclidean distance between models is not very meaningful. To remedy this issue, we can develop heuristic algorithms that resembles the form of FEDAMP but incorporate favorable measure of similarity. As an example, one may use the popular cosine similarity to measure the similarity between models, which is defined as  $\cos(x, y) = (x/\|x\|)^T(y/\|y\|)$ . In addition, to improve the effectiveness of attention, we compose it with an exponential function, resulting in a non-negative similarity function  $s(x, y) = e^{\sigma \cos(x, y)}$  for some  $\sigma > 0$ . Moreover, we further allow the self-attention parameters  $\{\tau_{k,i}\}$  in (7) and the local training parameters  $\{\beta_k\}$  in (5) to be customized by the clients. The obtained heuristic algorithm is summarized in Algorithm 2. Its convergence guarantee is unclear, but we will demonstrate its strong empirical performance in Sec. 4.

### 3.4 Convergence Analysis of FEDAMP

In this subsection, we provide the non-asymptotic convergence guarantee of the general framework FEDAMP for both convex and non-convex  $\mathcal{G}$  in (1) under suitable conditions. Denote by  $\partial\mathcal{F}$  the subdifferential of  $\mathcal{F}$  [45]. We first introduce the following assumption.

**Assumption 1** *There exists a constant  $B > 0$  such that for every  $k$ ,*

$$\max\{\|Y\| : Y \in \partial\mathcal{F}(w_1^k, \dots, w_m^k)\} \leq B, \quad \|\nabla\mathcal{D}(w_1^k, \dots, w_m^k)\| \leq B/\lambda. \quad (12)$$

Assumption 1 is widely used in the study of incremental and stochastic optimization algorithms; see, e.g., [40, 46]. It holds if both  $\mathcal{F}$  and  $\mathcal{D}$  are locally Lipschitz and the sequence of personalized models  $(w_1^k, \dots, w_m^k)$  are bounded for all  $k$ .

When both  $\mathcal{F}$  and  $\mathcal{D}$  are convex, we have the following guarantee of FEDAMP.

**Theorem 1** *Suppose that Assumption 1 holds and that  $\mathcal{F}$  and  $\mathcal{D}$  in (1) are convex. In addition, suppose that  $\alpha_k = \lambda/\sqrt{K}$  and  $\beta_k = 1/\sqrt{K}$  for all  $k$ , where  $K$  is the total number of communication rounds. Then, the sequence  $\{(w_1^k, \dots, w_m^k)\}$  generated by Algorithm 1 satisfies*

$$\min_{0 \leq k \leq K} \mathcal{G}(w_1^k, \dots, w_m^k) \leq \mathcal{G}^* + \frac{\sum_{i=1}^m \|w_i^0 - w_i^*\|^2 + 5B^2}{\sqrt{K}}, \quad (13)$$

where  $\mathcal{G}^*$  is the optimal value and  $(w_1^*, \dots, w_m^*)$  is an optimal solution of (1).

Next, we provide the guarantee of FEDAMP for the case where  $\mathcal{G}$  is smooth and non-convex. Recall that  $\partial\mathcal{F}(W) = \{\nabla\mathcal{F}(W)\}$  if  $\mathcal{F}$  is differentiable at  $W$ .

**Theorem 2** *Suppose that Assumption 1 holds and that  $\mathcal{F}$  and  $\mathcal{D}$  in (1) are continuously differentiable with  $\nabla\mathcal{F}$  and  $\nabla\mathcal{D}$  being Lipschitz continuous with modulus  $L$ . In addition, suppose that  $\alpha_k = \lambda/\sqrt{K}$  and  $\beta_k = 1/\sqrt{K}$  for all  $k$ , where  $K$  is the total number of communication rounds. Then, the sequence  $\{(w_1^k, \dots, w_m^k)\}$  generated by Algorithm 1 satisfies*

$$\min_{0 \leq k \leq K} \|\nabla\mathcal{G}(w_1^k, \dots, w_m^k)\|^2 \leq \frac{18(\mathcal{G}(w_1^0, \dots, w_m^0) - \mathcal{G}^* + 20LB^2)}{\sqrt{K}} + \mathcal{O}\left(\frac{1}{K}\right) \quad (14)$$

where  $\mathcal{G}^*$  is the optimal value of (1).

## 4 Experiments

In this section, we empirically demonstrate the outstanding performance of FEDAMP and HEURFEDAMP in a challenging non-IID data setting (Sec. 4.2). We also evaluate the performance of our methods under more practical scenarios such as dirty labels (Sec. 4.3). Due to the limitation of the paper length, we only include the key experiment results in this section and more extensive results are provided in the supplemental material, including the experiments on dropped clients.

### 4.1 Experimental Details

**Baselines.** We compare the state of arts global federated learning algorithms, i.e., FedAvg [2] and FedProx [3], as well as their extensions for local customization by finetuning the global model on client, which are named as FedAvg-FT

and FedProx-FT, respectively. In addition, we also report the results of separate training since its performance is the lower bound for the local models.

**Datasets.** We use four datasets in our experiments: MNIST [47], FMNIST (Fashion-MNIST) [48], EMNIST (Extended-MNIST) [49], and CIFAR100 [50]. We describe how we prepare EMNIST dataset here and leave the similar preparation details for the rest datasets in supplemental material.

We first set up 62 clients and divide them into three groups. The first group contains 10 clients (client 0-9), where each client has 1000 training samples dominated by the digits classes ('0' to '9'). The second group contains 26 clients (client 10-35), where each client has 700 training samples dominated by the upper-case letters classes ('A' to 'Z'). The third group also contains 26 clients (client 36-61), where each client has 400 training samples dominated by the lower-case letters classes ('a' to 'z'). In addition, each client has 100 testing samples. On each client, the dominated classes uniformly have 80% of data while the non-dominated classes uniformly have the rest 20% data.

Comparing with the pathological non-IID setting [2], every client in our non-IID setting has data from all classes and the number of samples on each client is unbalanced. Moreover, in order to facilitate a more practical setting, we consider the scenario that some clients have incorrect annotations in the training data in Sec. 4.3.

**Implementation.** We implement separate training and our proposed methods (i.e., FEDAMP and HEURFEDAMP) in Pytorch. We also extend the implementations of FedAvg and FedProx in Tensorflow from [3]. For MNIST, FMNIST and EMNIST datasets, we use the same CNN architecture as [2], where as for CIFAR100, we use ResNet18 from [51]. In addition, we employ ADAM [52] with a learning rate  $10^{-3}$  as the optimization algorithm for the local training on each client. To make a fair comparison among all the compared methods, experiments are set the batch size as 100 and the number of epochs as 10 in each round of the local training. The more detailed hyperparameters are given in the supplemental material.

## 4.2 Inter-client Collaboration Effect

Table 1: Best mean validation accuracy (in %)

Methods	MNIST	FMNIST	EMNIST	CIFAR100
Separate	86.30	86.73	61.78	39.99
FedAvg	81.82	79.50	72.27	35.21
FedAvg-FT	91.79	89.73	78.93	49.00
FedProx	81.46	78.71	70.55	37.31
FedProx-FT	94.10	87.51	77.31	50.24
FEDAMP	<b>97.59</b>	90.97	81.22	53.04
HEURFEDAMP	97.36	<b>91.37</b>	<b>81.47</b>	<b>53.27</b>

The performance of FEDAMP and HEURFEDAMP comparing with baselines are shown in Table 1. In this table, we report the best mean validation accuracy across all the clients during the federated training. Based on Wilcoxon signed-rank test [53], both FEDAMP and HEURFEDAMP significantly ( $P \leq 10^{-4}$ ) outperform all baselines.

The reason for superior performance of our methods is the success of attentive collaboration mechanism among clients. As a result, each client has its own personalized cloud model, whose performance benefits from the clients with the similar distribution, while minimizing the harm induced by those with different distributions. This phenomenon can be observed from Fig. 1, which shows the pattern of the linear combination weights  $\xi_{ij}$  defined in (6) from the round achieving the best mean validation accuracy for EMNIST dataset. As explained in Sec. 2, only one global model is constructed by FedAvg and FedProx on the cloud. Thus, the linear combination weights for computing this model respect to each client are same, i.e.,  $\xi_{ij} = N_i / (\sum_{i=1}^m N_i)$  for all  $i$ , where  $N_i$  is the number of samples on client  $i$ . We draw the pattern of  $\xi$  for FedAvg and FedProx in Fig. 1a. However, due to the attentive collaboration mechanism caused by (9) and (10), the linear combination weights for computing the personalized cloud models in FEDAMP and HEURFEDAMP are different. We draw the pattern of  $\xi$  for FEDAMP and HEURFEDAMP in Fig. 1b and Fig. 1c, respectively. In addition, the patterns of aggregation weights of FEDAMP and HEURFEDAMP are consistent with the data distribution as expected. For example, the upper-case letters group (i.e., client 10-35) only collaborates within the group while has non-collaboration with the other two groups of the clients. This implies FEDAMP and HEURFEDAMP have found the correct inter-client collaboration and clearly explains the advantages of constructing personalized cloud models for each client over a single cloud model for all clients.

## 4.3 Tolerance to Dirty Data

We further explore the advantages of attentive collaboration mechanism by comparing FEDAMP and HEURFEDAMP with the baselines on a more practical scenario, where the training data on some clients are contaminated by dirty

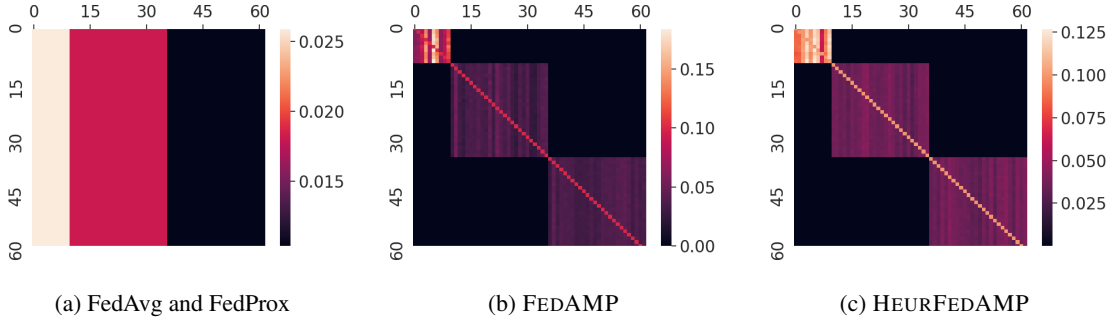


Figure 1: Patterns of aggregation weights  $\xi$  for computing the cloud models respect to each client

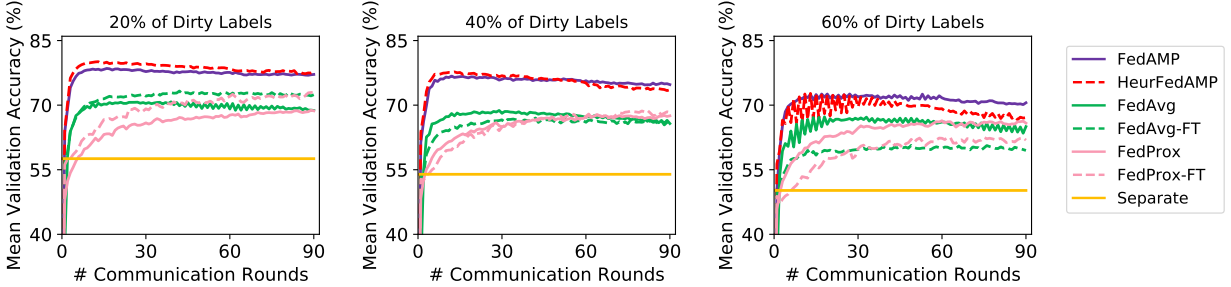


Figure 2: Performance of FEDAMP and HEURFEDAMP compared with baselines for different levels of dirty labels on EMNIST.

labels. This phenomenon is quite usual because the quality of annotations is not always good enough. To conduct this experiment, we set two out of five clients have dirty labels, and three levels are considered, where percentages of dirty labels are set as 20%, 40% and 60%, respectively. We show the results of EMNIST dataset in Fig. 2 and more results are in the supplemental material. Fig. 2 illustrates that by leveraging the attentive message passing mechanism, FEDAMP and HEURFEDAMP obviously outperform all other compared approaches in all levels of dirty labels in terms of the mean validation accuracy. In addition, it is worthy to notice that HEURFEDAMP is less stable as the level of dirty labels grows since there is no convergence guarantee for this heuristic method as stated in Sec. 3.3.

## 5 Conclusion

In this paper, we tackle the challenging personalized federated learning problem by FEDAMP and HEURFEDAMP that realize a highly useful attentive collaboration mechanism to significantly boost the collaboration effectiveness between clients without infringing their data privacy. We theoretically analyzed how the attentive collaboration mechanism encourages clients with similar models to have much stronger collaboration than clients with dissimilar models, and empirically demonstrated that this mechanism significantly boosts the learning performance by adaptively discovering the underlying collaboration relationships between clients. As future work, we will extend FEDAMP and HEURFEDAMP to conduct more effective attentive collaboration with lower communication cost.

## Acknowledgements

Most of the work of the author Z. Zhou was done when he was affiliated with the Department of Mathematics of Hong Kong Baptist University (HKBU) and was supported in part by an HKBU Start-up Grant.

## References

- [1] Jacob Poushter. Smartphone ownership and internet usage continues to climb in emerging economies. *Pew Research Center*, 22:1–44, 2016.
- [2] H Brendan McMahan, Eider Moore, Daniel Ramage, Seth Hampson, et al. Communication-efficient learning of deep networks from decentralized data. In *International Conference on Artificial Intelligence and Statistics*, pages 1273–1282, 2016.



- [3] Tian Li, Anit Kumar Sahu, Manzil Zaheer, Maziar Sanjabi, Ameet Talwalkar, and Virginia Smith. Federated optimization in heterogeneous networks. In *Machine Learning and Systems*, pages 429–450, 2020.
- [4] Yue Zhao, Meng Li, Liangzhen Lai, Naveen Suda, Damon Civin, and Vikas Chandra. Federated learning with non-iid data. *arXiv preprint arXiv:1806.00582*, 2018.
- [5] Úlfar Erlingsson, Vasyi Pihur, and Aleksandra Korolova. Rappor: Randomized aggregatable privacy-preserving ordinal response. In *ACM SIGSAC Conference on Computer and Communications Security*, pages 1054–1067, 2014.
- [6] Andrew Hard, Kanishka Rao, Rajiv Mathews, Swaroop Ramaswamy, Françoise Beaufays, Sean Augenstein, Hubert Eichner, Chloé Kiddon, and Daniel Ramage. Federated learning for mobile keyboard prediction. *arXiv preprint arXiv:1811.03604*, 2018.
- [7] Timothy Yang, Galen Andrew, Hubert Eichner, Haicheng Sun, Wei Li, Nicholas Kong, Daniel Ramage, and Françoise Beaufays. Applied federated learning: Improving google keyboard query suggestions. *arXiv preprint arXiv:1812.02903*, 2018.
- [8] Peter Kairouz, H Brendan McMahan, Brendan Avent, Aurélien Bellet, Mehdi Bennis, Arjun Nitin Bhagoji, Keith Bonawitz, Zachary Charles, Graham Cormode, Rachel Cummings, et al. Advances and open problems in federated learning. *arXiv preprint arXiv:1912.04977*, 2019.
- [9] Alireza Fallah, Aryan Mokhtari, and Asuman Ozdaglar. Personalized federated learning: A meta-learning approach. *arXiv preprint arXiv:2002.07948*, 2020.
- [10] Yishay Mansour, Mehryar Mohri, Jae Ro, and Ananda Theertha Suresh. Three approaches for personalization with applications to federated learning. *arXiv preprint arXiv:2002.10619*, 2020.
- [11] Johannes Schneider and Michail Vlachos. Mass personalization of deep learning. In *International Data Science Conference*, 2020.
- [12] Kangkang Wang, Rajiv Mathews, Chloé Kiddon, Hubert Eichner, Françoise Beaufays, and Daniel Ramage. Federated evaluation of on-device personalization. *arXiv preprint arXiv:1910.10252*, 2019.
- [13] Yuyang Deng, Mohammad Mahdi Kamani, and Mehrdad Mahdavi. Adaptive personalized federated learning. *arXiv preprint arXiv:2003.13461*, 2020.
- [14] Filip Hanzely and Peter Richtárik. Federated learning of a mixture of global and local models. *arXiv preprint arXiv:2002.05516*, 2020.
- [15] Alex Nichol, Joshua Achiam, and John Schulman. On first-order meta-learning algorithms. *arXiv preprint arXiv:1803.02999*, 2018.
- [16] Fei Chen, Zhenhua Dong, Zhenguo Li, and Xiuqiang He. Federated meta-learning for recommendation. *arXiv preprint arXiv:1802.07876*, 2018.
- [17] Shaoxiong Ji, Shirui Pan, Guodong Long, Xue Li, Jing Jiang, and Zi Huang. Learning private neural language modeling with attentive aggregation. In *IEEE International Joint Conference on Neural Networks*, pages 1–8, 2019.
- [18] Mikhail Yurochkin, Mayank Agarwal, Soumya Ghosh, Kristjan Greenewald, Nghia Hoang, and Yasaman Khazaeni. Bayesian nonparametric federated learning of neural networks. In *International Conference on Machine Learning*, pages 7252–7261, 2019.
- [19] Hongyi Wang, Mikhail Yurochkin, Yuekai Sun, Dimitris Papailiopoulos, and Yasaman Khazaeni. Federated learning with matched averaging. In *International Conference on Learning Representations*, 2020.
- [20] Yishay Mansour, Mehryar Mohri, and Afshin Rostamizadeh. Domain adaptation: Learning bounds and algorithms. *arXiv preprint arXiv:0902.3430*, 2009.
- [21] Corinna Cortes and Mehryar Mohri. Domain adaptation and sample bias correction theory and algorithm for regression. *Theoretical Computer Science*, 519:103–126, 2014.
- [22] Shai Ben-David, John Blitzer, Koby Crammer, Alex Kulesza, Fernando Pereira, and Jennifer Wortman Vaughan. A theory of learning from different domains. *Machine Learning*, 79(1-2):151–175, 2010.
- [23] Mikhail Khodak, Maria-Florina F Balcan, and Ameet S Talwalkar. Adaptive gradient-based meta-learning methods. In *Advances in Neural Information Processing Systems*, pages 5915–5926, 2019.
- [24] Yihan Jiang, Jakub Konečný, Keith Rush, and Sreeram Kannan. Improving federated learning personalization via model agnostic meta learning. *arXiv preprint arXiv:1909.12488*, 2019.
- [25] Viraj Kulkarni, Milind Kulkarni, and Aniruddha Pant. Survey of personalization techniques for federated learning. *arXiv preprint arXiv:2003.08673*, 2020.

- [26] Andreas Argyriou, Theodoros Evgeniou, and Massimiliano Pontil. Multi-task feature learning. In *Advances in Neural Information Processing Systems*, pages 41–48, 2007.
- [27] Jianhui Chen, Jiayu Zhou, and Jieping Ye. Integrating low-rank and group-sparse structures for robust multi-task learning. In *ACM SIGKDD International Conference on Knowledge Discovery and Data Mining*, pages 42–50, 2011.
- [28] Theodoros Evgeniou and Massimiliano Pontil. Regularized multi-task learning. In *ACM SIGKDD International Conference on Knowledge Discovery and Data Mining*, pages 109–117, 2004.
- [29] Seyoung Kim and Eric P Xing. Statistical estimation of correlated genome associations to a quantitative trait network. *PLOS Genetics*, 5(8), 2009.
- [30] André R Gonçalves, Fernando J Von Zuben, and Arindam Banerjee. Multi-task sparse structure learning with gaussian copula models. *The Journal of Machine Learning Research*, 17(1):1205–1234, 2016.
- [31] Laurent Jacob, Jean-philippe Vert, and Francis R Bach. Clustered multi-task learning: A convex formulation. In *Advances in Neural Information Processing Systems*, pages 745–752, 2009.
- [32] Yu Zhang and Dit-Yan Yeung. A convex formulation for learning task relationships in multi-task learning. In *Conference on Uncertainty in Artificial Intelligence*, pages 733–742, 2012.
- [33] Paul Vanhaesebrouck, Aurélien Bellet, and Marc Tommasi. Decentralized collaborative learning of personalized models over networks. In *International Conference on Artificial Intelligence and Statistics*, pages 509–517, 2017.
- [34] Aurélien Bellet, Rachid Guerraoui, Mahsa Taziki, and Marc Tommasi. Personalized and private peer-to-peer machine learning. In *International Conference on Artificial Intelligence and Statistics*, pages 473–481, 2018.
- [35] Valentina Zantedeschi, Aurelien Bellet, and Marc Tommasi. Fully decentralized joint learning of personalized models and collaboration graphs. In *International Conference on Artificial Intelligence and Statistics*, 2020.
- [36] Liyang Xie, Inci M Baytas, Kaixiang Lin, and Jiayu Zhou. Privacy-preserving distributed multi-task learning with asynchronous updates. In *ACM SIGKDD International Conference on Knowledge Discovery and Data Mining*, pages 1195–1204, 2017.
- [37] Virginia Smith, Chao-Kai Chiang, Maziar Sanjabi, and Ameet S Talwalkar. Federated multi-task learning. In *Advances in Neural Information Processing Systems*, pages 4424–4434, 2017.
- [38] Lei Han and Yu Zhang. Learning multi-level task groups in multi-task learning. In *AAAI Conference on Artificial Intelligence*, 2015.
- [39] Yu Zhang and Qiang Yang. A survey on multi-task learning. *arXiv preprint arXiv:1707.08114*, 2017.
- [40] Dimitri P Bertsekas. Incremental gradient, subgradient, and proximal methods for convex optimization: A survey. *Optimization for Machine Learning*, 2010(1-38):3, 2011.
- [41] R Tyrrell Rockafellar. Monotone operators and the proximal point algorithm. *SIAM Journal on Control and Optimization*, 14(5):877–898, 1976.
- [42] Jianqing Fan and Runze Li. Variable selection via nonconcave penalized likelihood and its oracle properties. *Journal of the American Statistical Association*, 96(456):1348–1360, 2001.
- [43] Cun-Hui Zhang. Nearly unbiased variable selection under minimax concave penalty. *The Annals of Statistics*, 38(2):894–942, 2010.
- [44] Jean-Philippe Vert, Koji Tsuda, and Bernhard Schölkopf. A primer on kernel methods. *Kernel Methods in Computational Biology*, 47:35–70, 2004.
- [45] R Tyrrell Rockafellar and Roger J-B Wets. *Variational Analysis*, volume 317. Springer Science & Business Media, 2009.
- [46] Arkadi Nemirovski, Anatoli Juditsky, Guanghui Lan, and Alexander Shapiro. Robust stochastic approximation approach to stochastic programming. *SIAM Journal on optimization*, 19(4):1574–1609, 2009.
- [47] Yann LeCun, Corinna Cortes, and CJ Burges. Mnist handwritten digit database. 2010.
- [48] Han Xiao, Kashif Rasul, and Roland Vollgraf. Fashion-mnist: a novel image dataset for benchmarking machine learning algorithms. *arXiv preprint arXiv:1708.07747*, 2017.
- [49] Gregory Cohen, Saeed Afshar, Jonathan Tapson, and Andre Van Schaik. Emnist: Extending mnist to handwritten letters. In *IEEE International Joint Conference on Neural Networks*, pages 2921–2926, 2017.
- [50] Alex Krizhevsky and Geoffrey Hinton. Learning multiple layers of features from tiny images. *Technical Report, University of Toronto*, 2009.
- [51] Kaiming He, Xiangyu Zhang, Shaoqing Ren, and Jian Sun. Deep residual learning for image recognition. In *IEEE Conference on Computer Vision and Pattern Recognition*, June 2016.

- [52] Diederik P Kingma and Jimmy Ba. Adam: A method for stochastic optimization. In *International Conference on Learning Representations*, 2015.
- [53] Frank Wilcoxon. Individual comparisons by ranking methods. In *Breakthroughs in Statistics*, pages 196–202. Springer, 1992.
- [54] Xiao Li, Zhihui Zhu, Anthony Man-Cho So, and Jason D Lee. Incremental methods for weakly convex optimization. *arXiv preprint arXiv:1907.11687*, 2019.
- [55] Yurii Nesterov. *Introductory lectures on convex optimization: A basic course*, volume 87. Springer Science & Business Media, 2013.

## Supplementary Material

In this supplementary material, we provide the proofs for Theorem 1 and 2 in Sec. A and B, respectively. In addition, we show more extensive experimental results in Sec. C.

### A Proof of Theorem 1

Throughout the proof, we denote by  $\mathcal{G}^*$  the optimal value and  $W^*$  an optimal solution of problem (1). Recall that if  $\beta_k = \alpha_k/\lambda$  for all  $k$ , FEDAMP follows the update formula (2) and (3). Since  $\mathcal{F}$  is convex, the objective function in (3) is strongly convex with modulus  $\lambda/\alpha_k$ . This, together with the fact that  $W^k$  is the optimal solution of (3), implies that

$$\mathcal{F}(W^k) + \frac{\lambda}{2\alpha_k} \|W^k - U^k\|^2 \leq \mathcal{F}(W^*) + \frac{\lambda}{2\alpha_k} \|W^* - U^k\|^2 - \frac{\lambda}{2\alpha_k} \|W^* - W^k\|^2.$$

Upon rearrangement, we obtain

$$\|W^k - W^*\|^2 \leq \|U^k - W^*\|^2 - \frac{2\alpha_k}{\lambda} (\mathcal{F}(W^k) - \mathcal{F}(W^*)). \quad (15)$$

Since  $U^k$  is generated by (2), we have

$$\begin{aligned} \|U^k - W^*\|^2 &= \|W^{k-1} - \alpha_k \nabla \mathcal{D}(W^{k-1}) - W^*\|^2 \\ &= \|W^{k-1} - W^*\|^2 - 2\alpha_k \langle \nabla \mathcal{D}(W^{k-1}), W^{k-1} - W^* \rangle + \alpha_k^2 \|\nabla \mathcal{D}(W^{k-1})\|^2. \end{aligned}$$

Besides, since  $\mathcal{D}$  is convex, one has

$$\mathcal{D}(W^*) \geq \mathcal{D}(W^{k-1}) + \langle \nabla \mathcal{D}(W^{k-1}), W^* - W^{k-1} \rangle$$

By combining the above two inequalities and using Assumption 1, we obtain

$$\|U^k - W^*\|^2 \leq \|W^{k-1} - W^*\|^2 - 2\alpha_k (\mathcal{D}(W^{k-1}) - \mathcal{D}(W^*)) + \frac{\alpha_k^2 B^2}{\lambda^2} \quad (16)$$

Substituting (16) into (15) and using the definition  $\mathcal{G} = \mathcal{F} + \lambda \mathcal{D}$  yield

$$\|W^k - W^*\|^2 \leq \|W^{k-1} - W^*\|^2 - \frac{2\alpha_k}{\lambda} (\mathcal{F}(W^k) + \lambda \mathcal{D}(W^{k-1}) - \mathcal{G}^*) + \frac{\alpha_k^2 B^2}{\lambda^2}. \quad (17)$$

Moreover, by the convexity of  $\mathcal{F}$  and Assumption 1, we have, with any  $Y \in \partial \mathcal{F}(W^{k-1})$ , that

$$\mathcal{F}(W^k) - \mathcal{F}(W^{k-1}) \geq \langle Y, W^k - W^{k-1} \rangle \geq -\|Y\| \|W^k - W^{k-1}\| \geq -B \|W^k - W^{k-1}\|.$$

Also, it follows from the optimality condition of (3) that

$$0 = \tilde{\nabla} \mathcal{F}(W^k) + \frac{\lambda}{\alpha_k} (W^k - U^k)$$

for some  $\tilde{\nabla} \mathcal{F}(W^k) \in \partial \mathcal{F}(W^k)$ , which, together with (2) and Assumption 1, yields

$$\|W^k - W^{k-1}\| = \left\| U^k - \frac{\alpha_k}{\lambda} \tilde{\nabla} \mathcal{F}(W^k) - W^{k-1} \right\| = \left\| \alpha_k \nabla \mathcal{D}(W^{k-1}) + \frac{\alpha_k}{\lambda} \tilde{\nabla} \mathcal{F}(W^k) \right\| \leq \frac{2\alpha_k B}{\lambda}.$$

Upon combining the above two inequalities, we obtain

$$\mathcal{F}(W^k) \geq \mathcal{F}(W^{k-1}) - \frac{2\alpha_k B^2}{\lambda}.$$

Substituting this into (17) and using the definition  $\mathcal{G} = \mathcal{F} + \lambda \mathcal{D}$  yield

$$\|W^k - W^*\|^2 \leq \|W^{k-1} - W^*\|^2 - \frac{2\alpha_k}{\lambda} (\mathcal{G}(W^{k-1}) - \mathcal{G}^*) + \frac{5\alpha_k^2 B^2}{\lambda^2},$$

which, after rearrangement, leads to

$$\mathcal{G}(W^{k-1}) - \mathcal{G}^* \leq \frac{\lambda}{2\alpha_k} \|W^{k-1} - W^*\|^2 - \frac{\lambda}{2\alpha_k} \|W^k - W^*\|^2 + \frac{5\alpha_k B^2}{2\lambda}.$$

Recall that  $\alpha_k = \alpha = \lambda/\sqrt{K}$  for all  $k$ . Then, by summing up the above inequality from  $k = 1$  to  $k = K$ , we obtain

$$K \cdot \left( \min_{0 \leq k \leq K-1} \mathcal{G}(W^k) - \mathcal{G}^* \right) \leq \sum_{k=0}^{K-1} \mathcal{G}(W^k) - \mathcal{G}^* \leq \frac{\lambda}{2\alpha} \|W^0 - W^*\|^2 + \frac{5K\alpha B^2}{2\lambda}.$$

Upon deviding both sides of the above inequality by  $K$  and using  $\alpha = \lambda/\sqrt{K}$  for all  $k$ , we obtain the desired result (13).

## B Proof of Theorem 2

The proof of Theorem 2 is motivated by the analysis in [54]. Define the function  $\hat{\mathcal{G}} : \mathbb{R}^d \rightarrow \mathbb{R}$  as

$$\hat{\mathcal{G}}(W) = \min_{V \in \mathbb{R}^{d \times m}} \mathcal{G}(V) + 2L\|V - W\|^2, \quad (18)$$

where  $L$  is the Lipschitz constant of  $\nabla \mathcal{D}$ . Also, given any  $W \in \mathbb{R}^{d \times m}$ , we denote by  $\bar{W}$  an optimal solution of the minimization problem in (18), i.e.,  $\hat{\mathcal{G}}(W) = \mathcal{G}(\bar{W}) + 2L\|\bar{W} - W\|^2$ . It then follows from the update of  $U^k$  in (2) that

$$\begin{aligned} \hat{\mathcal{G}}(U^k) &= \min_V \mathcal{G}(V) + 2L\|V - U^k\|^2 \leq \mathcal{G}(\bar{W}^{k-1}) + 2L\|\bar{W}^{k-1} - U^k\|^2 \\ &= \mathcal{G}(\bar{W}^{k-1}) + 2L\|\bar{W}^{k-1} - W^{k-1} + \alpha_k \nabla \mathcal{D}(W^{k-1})\|^2 \\ &= \mathcal{G}(\bar{W}^{k-1}) + 2L\|\bar{W}^{k-1} - W^{k-1}\|^2 + 4\alpha_k L \langle \nabla \mathcal{D}(W^{k-1}), \bar{W}^{k-1} - W^{k-1} \rangle + 2\alpha_k^2 L \|\nabla \mathcal{D}(W^{k-1})\|^2 \\ &= \hat{\mathcal{G}}(W^{k-1}) + 4\alpha_k L \langle \nabla \mathcal{D}(W^{k-1}), \bar{W}^{k-1} - W^{k-1} \rangle + 2\alpha_k^2 L \|\nabla \mathcal{D}(W^{k-1})\|^2. \end{aligned}$$

By Assumption 1, we have  $\|\nabla \mathcal{D}(W^{k-1})\| \leq B/\lambda$ . Besides, since  $\nabla \mathcal{D}$  is Lipschitz continuous with Lipschitz constant  $L/\lambda$ , it holds that

$$\mathcal{D}(\bar{W}^{k-1}) - \mathcal{D}(W^{k-1}) - \langle \nabla \mathcal{D}(W^{k-1}), \bar{W}^{k-1} - W^{k-1} \rangle \geq -\frac{L}{2\lambda} \|\bar{W}^{k-1} - W^{k-1}\|^2,$$

see, e.g., [55]. Thus, we obtain

$$\hat{\mathcal{G}}(U^k) \leq \hat{\mathcal{G}}(W^{k-1}) + 4\alpha_k L (\mathcal{D}(\bar{W}^{k-1}) - \mathcal{D}(W^{k-1})) + \frac{2\alpha_k L^2}{\lambda} \|\bar{W}^{k-1} - W^{k-1}\|^2 + \frac{2\alpha_k^2 L B^2}{\lambda^2}. \quad (19)$$

Moreover, by the update of  $W^k$  in (3) and the fact that  $\mathcal{F}$  is continuously differentiable, we know that

$$\nabla \mathcal{F}(W^k) + \frac{\lambda}{\alpha_k} (W^k - U^k) = 0. \quad (20)$$

This, together with (18), yields

$$\begin{aligned} \hat{\mathcal{G}}(W^k) &= \min_V \mathcal{G}(V) + 2L\|V - W^k\|^2 \leq \mathcal{G}(\bar{U}^k) + 2L\|\bar{U}^k - W^k\|^2 \\ &= \mathcal{G}(\bar{U}^k) + 2L \left\| \bar{U}^k - U^k + \frac{\alpha_k}{\lambda} \nabla \mathcal{F}(W^k) \right\|^2 \\ &= \mathcal{G}(\bar{U}^k) + 2L \|\bar{U}^k - U^k\|^2 + \frac{4\alpha_k L}{\lambda} \langle \nabla \mathcal{F}(W^k), \bar{U}^k - U^k \rangle + \frac{2\alpha_k^2 L}{\lambda^2} \|\nabla \mathcal{F}(W^k)\|^2 \\ &= \hat{\mathcal{G}}(U^k) + \frac{4\alpha_k L}{\lambda} \langle \nabla \mathcal{F}(W^k), \bar{U}^k - W^k \rangle + \frac{4\alpha_k L}{\lambda} \langle \nabla \mathcal{F}(W^k), W^k - U^k \rangle + \frac{2\alpha_k^2 L}{\lambda^2} \|\nabla \mathcal{F}(W^k)\|^2 \\ &\leq \hat{\mathcal{G}}(U^k) + \frac{4\alpha_k L}{\lambda} \langle \nabla \mathcal{F}(W^k), \bar{U}^k - W^k \rangle + \frac{2\alpha_k^2 L}{\lambda^2} \|\nabla \mathcal{F}(W^k)\|^2, \end{aligned}$$

where the last inequality uses  $\langle \nabla \mathcal{F}(W^k), W^k - U^k \rangle \leq 0$ , which follows from (20). By Assumption 1, we have  $\|\nabla \mathcal{F}(W^k)\| \leq B$ . Besides, since  $\nabla \mathcal{F}$  is Lipschitz continuous with Lipschitz constant  $L$ , it holds that

$$\mathcal{F}(\bar{U}^k) - \mathcal{F}(W^k) - \langle \nabla \mathcal{F}(W^k), \bar{U}^k - W^k \rangle \geq -\frac{L}{2} \|\bar{U}^k - W^k\|^2.$$

Thus, we obtain

$$\hat{\mathcal{G}}(W^k) \leq \hat{\mathcal{G}}(U^k) + \frac{4\alpha_k L}{\lambda} (\mathcal{F}(\bar{U}^k) - \mathcal{F}(W^k)) + \frac{2\alpha_k L^2}{\lambda} \|\bar{U}^k - W^k\|^2 + \frac{2\alpha_k^2 L B^2}{\lambda^2}. \quad (21)$$

Next, we claim

$$\|\bar{W}^{k-1} - \bar{U}^k\| \leq 2\|W^{k-1} - U^k\| \leq \frac{2\alpha_k B}{\lambda}. \quad (22)$$

Indeed, by (18) and the definition of  $\bar{W}^{k-1}$  and  $\bar{U}^k$ , we have

$$\nabla \mathcal{G}(\bar{W}^{k-1}) + 4L(\bar{W}^{k-1} - W^{k-1}) = 0, \quad \nabla \mathcal{G}(\bar{U}^k) + 4L(\bar{U}^k - U^k) = 0,$$

which implies that

$$\langle \mathcal{G}(\bar{W}^{k-1}) - \mathcal{G}(\bar{U}^k), \bar{W}^{k-1} - \bar{U}^k \rangle = 4L \langle W^{k-1} - U^k, \bar{W}^{k-1} - \bar{U}^k \rangle - 4L \|\bar{W}^{k-1} - \bar{U}^k\|^2. \quad (23)$$

On the other hand, since  $\nabla\mathcal{F}$  and  $\nabla\mathcal{D}$  are Lipschitz continuous with constants  $L$  and  $L/\lambda$ , respectively, and  $\mathcal{G} = \mathcal{F} + \lambda\mathcal{D}$ , we know that  $\nabla\mathcal{G}$  is Lipschitz continuous with Lipschitz constant  $2L$ . It then follows that

$$\begin{aligned}\mathcal{G}(\bar{W}^{k-1}) - \mathcal{G}(\bar{U}^k) - \langle \nabla\mathcal{G}(\bar{U}^k), \bar{W}^{k-1} - \bar{U}^k \rangle &\geq -L\|\bar{W}^{k-1} - \bar{U}^k\|^2, \\ \mathcal{G}(\bar{U}^k) - \mathcal{G}(\bar{W}^{k-1}) - \langle \nabla\mathcal{G}(\bar{W}^{k-1}), \bar{U}^k - \bar{W}^{k-1} \rangle &\geq -L\|\bar{W}^{k-1} - \bar{U}^k\|^2,\end{aligned}$$

which, by adding up the two inequalities, yields

$$\langle \mathcal{G}(\bar{W}^{k-1}) - \mathcal{G}(\bar{U}^k), \bar{W}^{k-1} - \bar{U}^k \rangle \geq -2L\|\bar{W}^{k-1} - \bar{U}^k\|^2.$$

By this and (23), we obtain

$$\|\bar{W}^{k-1} - \bar{U}^k\|^2 \leq 2\langle W^{k-1} - U^k, \bar{W}^{k-1} - \bar{U}^k \rangle \leq 2\|W^{k-1} - U^k\| \|\bar{W}^{k-1} - \bar{U}^k\|$$

and thus the first inequality in (22) holds. The second inequality in (22) follows directly from (2) and Assumption 1. Besides, by (2), (3), and Assumption 1, we have

$$\|W^k - W^{k-1}\| = \left\| U^k - \frac{\alpha_k}{\lambda} \nabla\mathcal{F}(W^k) - W^{k-1} \right\| = \left\| \alpha_k \nabla\mathcal{D}(W^{k-1}) + \frac{\alpha_k}{\lambda} \nabla\mathcal{F}(W^k) \right\| \leq \frac{2\alpha_k B}{\lambda}. \quad (24)$$

Then, by (22), (24), the Lipschitz continuity of  $\nabla\mathcal{F}$ , and Assumption 1, we derive

$$\begin{aligned}\mathcal{F}(\bar{U}^k) - \mathcal{F}(W^k) &= \mathcal{F}(\bar{U}^k) - \mathcal{F}(\bar{W}^{k-1}) + \mathcal{F}(\bar{W}^{k-1}) - \mathcal{F}(W^{k-1}) + \mathcal{F}(W^{k-1}) - \mathcal{F}(W^k) \\ &\leq \mathcal{F}(\bar{W}^{k-1}) - \mathcal{F}(W^{k-1}) + B\|\bar{U}^k - \bar{W}^{k-1}\| + B\|W^{k-1} - W^k\| \\ &\leq \mathcal{F}(\bar{W}^{k-1}) - \mathcal{F}(W^{k-1}) + \frac{4\alpha_k B^2}{\lambda},\end{aligned}$$

and

$$\begin{aligned}\|\bar{U}^k - W^k\|^2 &= \|\bar{U}^k - \bar{W}^{k-1} + \bar{W}^{k-1} - W^{k-1} + W^{k-1} - W^k\|^2 \\ &\leq 4\|\bar{U}^k - \bar{W}^{k-1}\|^2 + 2\|\bar{W}^{k-1} - W^{k-1}\|^2 + 4\|W^{k-1} - W^k\|^2 \\ &\leq \frac{32\alpha_k^2 B^2}{\lambda^2} + 2\|\bar{W}^{k-1} - W^{k-1}\|^2,\end{aligned}$$

where we use the inequality  $(a + b + c)^2 \leq 2a^2 + 4b^2 + 4c^2$  for any  $a, b, c \in \mathbb{R}$ . Combining the above two inequalities with (21) gives us

$$\begin{aligned}\hat{\mathcal{G}}(W^k) &\leq \hat{\mathcal{G}}(U^k) + \frac{4\alpha_k L}{\lambda} (\mathcal{F}(\bar{W}^{k-1}) - \mathcal{F}(W^{k-1})) + \frac{4\alpha_k L^2}{\lambda} \|\bar{W}^{k-1} - W^{k-1}\|^2 \\ &\quad + \frac{18\alpha_k^2 L B^2}{\lambda^2} + \frac{64\alpha_k^3 L^2 B^2}{\lambda^3}.\end{aligned} \quad (25)$$

Upon adding (19) with (25) and using  $\mathcal{G} = \mathcal{F} + \lambda\mathcal{D}$ , we obtain

$$\begin{aligned}\hat{\mathcal{G}}(W^k) &\leq \hat{\mathcal{G}}(W^{k-1}) + \frac{4\alpha_k L}{\lambda} (\mathcal{G}(\bar{W}^{k-1}) - \mathcal{G}(W^{k-1})) + \frac{6\alpha_k L^2}{\lambda} \|\bar{W}^{k-1} - W^{k-1}\|^2 \\ &\quad + \frac{20\alpha_k^2 L B^2}{\lambda^2} + \frac{64\alpha_k^3 L^2 B^2}{\lambda^3} \\ &= \hat{\mathcal{G}}(W^{k-1}) + \frac{4\alpha_k L}{\lambda} (\mathcal{G}(\bar{W}^{k-1}) - \mathcal{G}(W^{k-1}) + 2L\|\bar{W}^{k-1} - W^{k-1}\|^2) \\ &\quad - \frac{2\alpha_k L^2}{\lambda} \|\bar{W}^{k-1} - W^{k-1}\|^2 + \frac{20\alpha_k^2 L B^2}{\lambda^2} + \frac{64\alpha_k^3 L^2 B^2}{\lambda^3}.\end{aligned} \quad (26)$$

By the definition of  $\bar{W}^{k-1}$  and (18), we know that  $\mathcal{G}(\bar{W}^{k-1}) + 2L\|\bar{W}^{k-1} - W^{k-1}\|^2 \leq \mathcal{G}(W^{k-1})$ . This, together with (26), yields

$$\hat{\mathcal{G}}(W^k) \leq \hat{\mathcal{G}}(W^{k-1}) - \frac{2\alpha_k L^2}{\lambda} \|\bar{W}^{k-1} - W^{k-1}\|^2 + \frac{20\alpha_k^2 L B^2}{\lambda^2} + \frac{64\alpha_k^3 L^2 B^2}{\lambda^3}.$$

Since  $\alpha_k = \alpha = \lambda/\sqrt{K}$  for all  $k = 1, 2, \dots, K$ , by summing up the above inequality from  $k = 1$  to  $k = K$ , we obtain

$$\begin{aligned}\min_{0 \leq k \leq K} \|\bar{W}^k - W^k\|^2 &\leq \frac{1}{K} \sum_{k=1}^K \|\bar{W}^{k-1} - W^{k-1}\|^2 \\ &\leq \frac{\lambda}{2\alpha L^2} \cdot \frac{\hat{\mathcal{G}}(W^0) - \hat{\mathcal{G}}(W^K)}{K} + \frac{10\alpha B^2}{\lambda L} + \frac{32\alpha^2 B^2}{\lambda^2}.\end{aligned} \quad (27)$$

From (18), one can verify that

$$\hat{\mathcal{G}}(W^0) \leq \mathcal{G}(W^0), \quad \text{and} \quad \hat{\mathcal{G}}(W^k) \geq \mathcal{G}^*,$$

where  $\mathcal{G}^*$  is the optimal value of (1). Also, using the definition of  $\bar{W}^k$ , we obtain by taking the optimality condition of (18) that

$$\nabla \mathcal{G}(\bar{W}^k) + 4L(\bar{W}^k - W^k) = 0,$$

which, together with the fact that  $\nabla \mathcal{G}$  is Lipschitz continuous with Lipschitz constant  $2L$ , implies that

$$\|\nabla \mathcal{G}(W^k)\| \leq \|\nabla \mathcal{G}(\bar{W}^k)\| + \|\nabla \mathcal{G}(\bar{W}^k) - \nabla \mathcal{G}(W^k)\| \leq 6L\|\bar{W}^k - W^k\|.$$

By these, (27), and  $\alpha = \lambda/\sqrt{K}$ , we have

$$\min_{0 \leq k \leq K} \|\nabla \mathcal{G}(W^k)\|^2 \leq \frac{18(\mathcal{G}(W^0) - \mathcal{G}^* + 20LB^2)}{\sqrt{K}} + \mathcal{O}\left(\frac{1}{K}\right) = \mathcal{O}\left(\frac{\mathcal{G}(w_1^0, \dots, w_m^0) - \mathcal{G}^* + LB^2}{\sqrt{K}}\right)$$

as desired.

## C Experiments

In this section, we provide more extensive experimental results to demonstrate the outstanding performance of FEDAMP and HEURFEDAMP in the challenging non-IID data setting as described in Sec. 4. Specifically, we show the results for dirty labels and dropped clients on different datasets for this setting in Sec. C.2 and C.3, respectively. In addition, we also provide experimental results on IID and pathological non-IID settings in Sec. C.4 and C.5, respectively.

### C.1 Experimental Details

**Datasets.** As detailed below, we describe how we prepare the challenging non-IID data settings for MNIST, FMNIST and CIFAR100 datasets, which is similar to the preparation for EMNIST as described in Sec. 4.1.

**MNIST:** We set 100 clients and divide them into 5 groups where each group contains 20 clients. Each client in the first group has 500 training samples, while for each client in the remaining 4 groups has 400, 300, 200 and 100 training samples, respectively. The training samples on each client in the first group are dominated by class ‘0’ to ‘1’, while for the training samples on each client in the remaining 4 groups, they are dominated by class ‘2’ to ‘3’, ‘4’ to ‘5’, ‘6’ to ‘7’, and ‘8’ to ‘9’, respectively. On each client, the dominated classes uniformly have 80% of data while the non-dominated classes uniformly have the rest 20% of data. In addition, each client has 100 testing samples which has the same distribution as the training samples on the same client.

**FMNIST:** For FMNIST dataset, we set the same preparation as the preparation for MNIST dataset except the number of training samples. Each client in the first group has 600 training samples, while for each client in the remaining 4 groups has 500, 400, 300 and 200 training samples, respectively. This is because the total number of FMNIST training samples is 60,000, and it is larger than the number of MNIST training samples which is 50,000.

**CIFAR100:** Since CIFAR100 originally has 100 classes which can be equally grouped into 20 superclasses, we divide this dataset into 20 groups where each group contains 5 clients. In each group, the training samples are dominated by one superclass. Similarly as before, on each client, the dominated classes uniformly have 80% of data while the non-dominated classes uniformly have the rest 20% of data. The number of training samples on client 1-20 (first 4 groups) is 500, while the number of training samples on client 21-40 (second 4 groups), 41-60 (third 4 groups), 61-80 (fourth 4 groups) and 81-100 (fifth 4 groups) is 400, 300, 200 and 100, respectively. In addition, each client has 100 testing samples which follow the distribution of the training samples on the same client.

For each dataset, besides the above challenging non-IID settings, we build two more types of data distribution settings, i.e., IID and pathological non-IID. In the IID setting, the data is uniformly distributed across different clients as described in [2], while in the pathological non-IID setting, we follow the steps provided in [2], where they partition the dataset based on labels and on each client, samples are drawn only from two classes. Comparing with the pathological non-IID setting, every client in the challenging non-IID setting has data from all classes and the number of samples on each client is unbalanced. This is a much more practical scenario to evaluate the federated learning algorithms’ performance on non-IID data settings.

**Implementation.** In Sec. 4.1, we provide the common hyperparameters used for all the methods in all the experiments. Here, we provide hyperparameters chosen for FEDAMP and HEURFEDAMP. First, we set  $\beta_k = 10^4$  initially and multiple it by 0.1 every 30 communication rounds for all the experiments. Second, from Table 2 to 4, we list all other hyperparameters which we obtain through the cross validation for each data setting. For the sake of simplicity, we choose a constant self-attention  $\tau_{k,i}$  in each training process, i.e.,  $\tau_{k,i} = \tau$ . We find that when  $\tau \approx 1 - 1/(N_i + 1)$  where

Table 2: Values of Hyperparameters(Chanllenging non-IID)

Parameter	MNIST	FMNIST	EMNIST	CIFAR100
$\sigma(\text{FEDAMP})$	100	10	10	$10^6$
$\sigma(\text{HEURFEDAMP})$	25	100	50	10
$\tau(\text{FEDAMP and HEURFEDAMP})$	0.95	0.95	0.9	0.8

Table 3: Values of Hyperparameters(IID)

Parameter	MNIST	FMNIST	EMNIST	CIFAR100
$\sigma(\text{FEDAMP})$	100	100	10	$10^6$
$\sigma(\text{HEURFEDAMP})$	25	50	50	10
$\tau(\text{FEDAMP and HEURFEDAMP})$	0.99	0.99	0.084	0.99

Table 4: Values of Hyperparameters(Pathological non-IID)

Parameter	MNIST	FMNIST	EMNIST	CIFAR100
$\sigma(\text{FEDAMP})$	100	10	10	$10^6$
$\sigma(\text{HEURFEDAMP})$	25	100	50	10
$\tau(\text{FEDAMP and HEURFEDAMP})$	0.5	0.5	0.5	0.5

$N_i$  is the number of similar distribution clients for client  $i$ , FEDAMP and HEURFEDAMP achieve better performance. We also observe that the parameter  $\sigma$ 's range for FEDAMP is very large due to the large variation of the Euclidean distance between parameters of two models in high dimension space. This is one of our motivations of proposing HEURFEDAMP in Sec. 3.3.

## C.2 Tolerance to Dirty Data

Besides the dirty data experiments on EMNIST dataset which is shown in Sec.4.3, we also conduct more experiments on MNIST, FMNIST and CIFAR100 to examine the tolerance of dirty data for FEDAMP, HEURFEDAMP, and baselines. The dirty data setting is the same as stated in Sec. 4.3.

The results on MNIST, FMNIST and CIFAR100 are shown in Fig. 3, 4 and 5, respectively. Similar to the performance on EMNIST which is shown in Sec. 4.3, FEDAMP and HEURFEDAMP all achieve the best mean validation accuracy in all three levels of dirty labels. This further confirms the effectiveness of applying the attentive message passing mechanism when encountering dirty data.

## C.3 Tolerance to Dropped Clients

To address the unreliable operating environment challenge in personalized federated learning, we conduct the dropped clients experiments for FEDAMP, HEURFEDAMP and the baselines. The results of 10%, 30%, and 50% randomly dropped clients in each round for the four challenging non-IID datasets are shown in Fig. 6 to 9. We clearly see that for EMNIST, MNIST and FMNIST, the overall mean validation accuracy of FEDAMP and HEURFEDAMP are better than baselines. For CIFAR100, FEDAMP and HEURFEDAMP can also compete or outperform FedAvg-FT in terms of the mean validation accuracy when the number of communication rounds is more than 60. This demonstrates that both FEDAMP and HEURFEDAMP can robustly handle clients dropping.

## C.4 Experiments results on the IID data setting

In Table 5, we summarize the performance of FEDAMP, HEURFEDAMP and baselines in terms of the best mean validation accuracy for the IID data setting described in Sec. C.1. We observe that for MNIST, FMNIST and EMNIST datasets, FEDAMP, HEURFEDAMP, FedAvg and FedProx all achieve similar accuracy. In the meanwhile, FedAvg outperforms other methods for CIFAR100 dataset. However, we find that by increasing the number of communication rounds for FEDAMP and HEURFEDAMP, they can achieve similar best mean validation accuracy as FedAvg for CIFAR100 dataset. One major reason for this observation is that in the IID setting, training a single global model is obviously more efficient than training multiple personalized cloud models. In conclusion, FEDAMP and HEURFEDAMP can achieve comparable performance as FedAvg and FedProx when data setting is IID but they may require a larger number of communication rounds to achieve the similar performance of FedAvg when encountering a difficult dataset, such as CIFAR100.



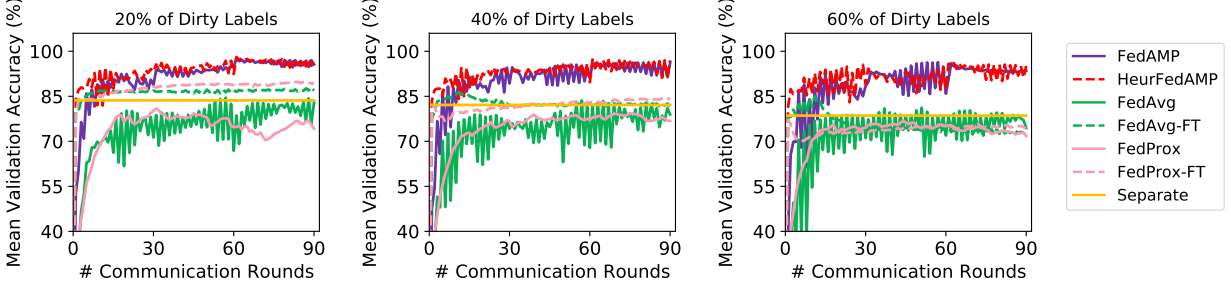


Figure 3: Performance of FEDAMP and HEURFEDAMP compared with baselines for different levels of dirty labels on MNIST.

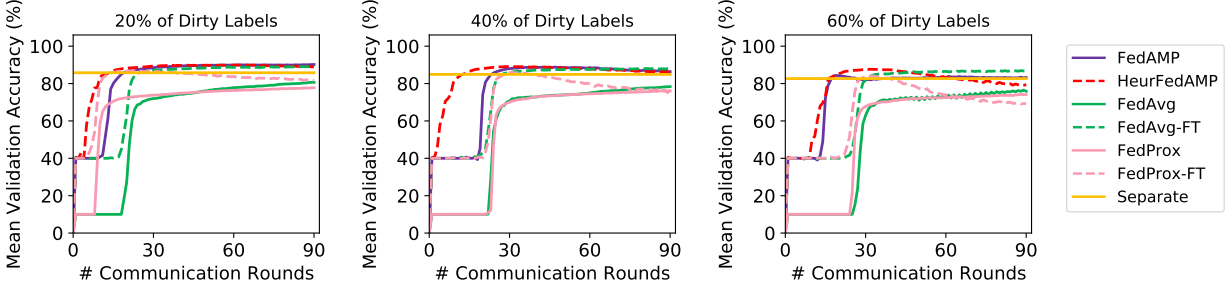


Figure 4: Performance of FEDAMP and HEURFEDAMP compared with baselines for different levels of dirty labels on FMNIST.

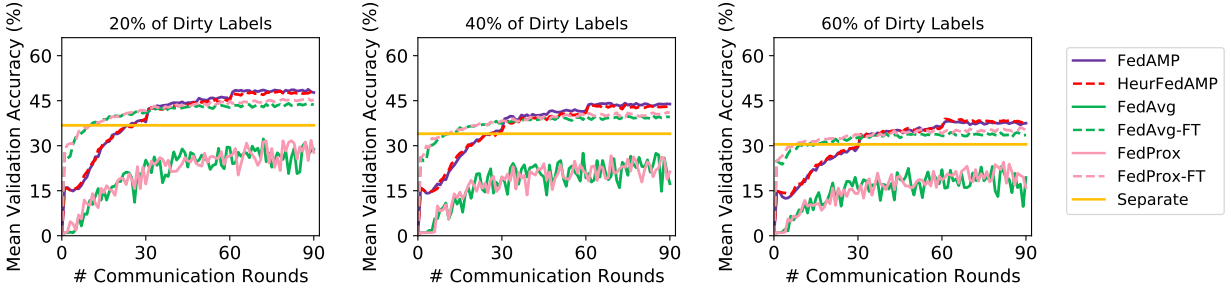


Figure 5: Performance of FEDAMP and HEURFEDAMP compared with baselines for different levels of dirty labels on CIFAR100.

Table 5: Best mean validation accuracy for IID (in %)

Methods	MNIST	FMNIST	EMNIST	CIFAR100
Separate	99.27	81.66	54.41	9.82
FedAvg	99.31	91.94	74.38	49.59
FedAvg-FT	98.98	90.17	70.53	35.07
FedProx	98.81	90.19	73.14	46.50
FedProx-FT	98.72	89.02	69.49	40.77
FEDAMP	99.22	92.05	74.07	45.58
HEURFEDAMP	99.28	91.80	74.07	45.88

**C.5 Experiments results on the pathological non-IID setting**

In Table 6, we summarize the performance of FEDAMP, HEURFEDAMP and baselines in terms of the best mean validation accuracy for the pathological non-IID data setting described in Sec. C.1. It is easy to observe that the FEDAMP, HEURFEDAMP, FedAvg-FT, Fedprox-FT and separate training all achieve over 97% best mean validation accuracy on MNIST, FMNIST and EMNIST datasets. For CIFAR100, FEDAMP, HEURFEDAMP, FedAvg-FT and Fedprox-FT all achieve around 95% accuracy which is about 2% higher than the separate training. In addition, we observe that in this pathological non-IID setting, the separate training can achieve much higher accuracy when comparing with other two data settings. The reason for these observations is that in this data setting, the samples on

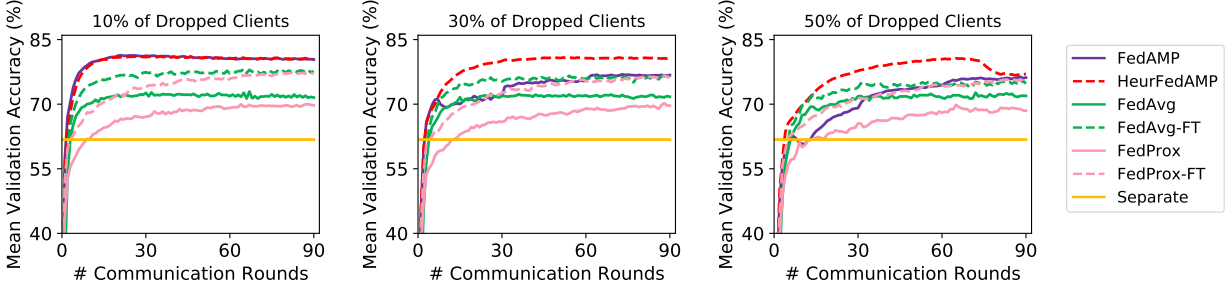


Figure 6: Performance of FEDAMP and HEURFEDAMP compared with baselines for different number of dropped clients on EMNIST.

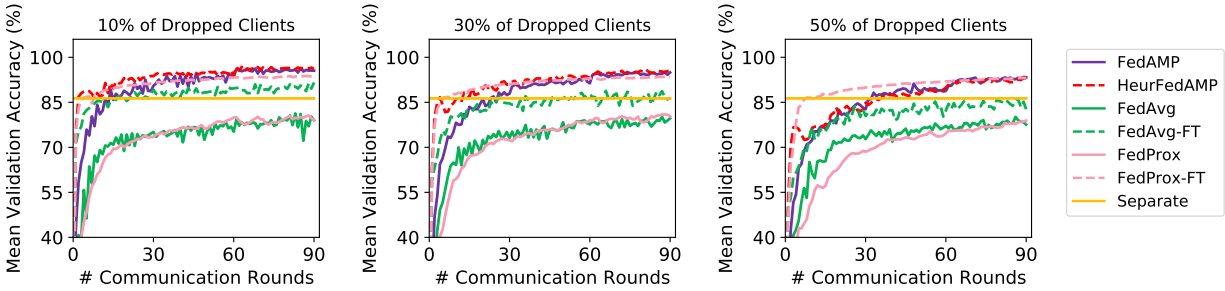


Figure 7: Performance of FEDAMP and HEURFEDAMP compared with baselines for different number of dropped clients on MNIST.

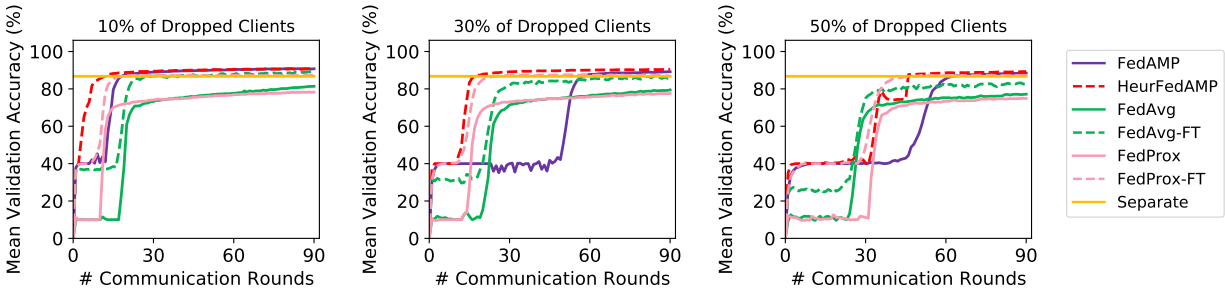


Figure 8: Performance of FEDAMP and HEURFEDAMP compared with baselines for different number of dropped clients on FMNIST.

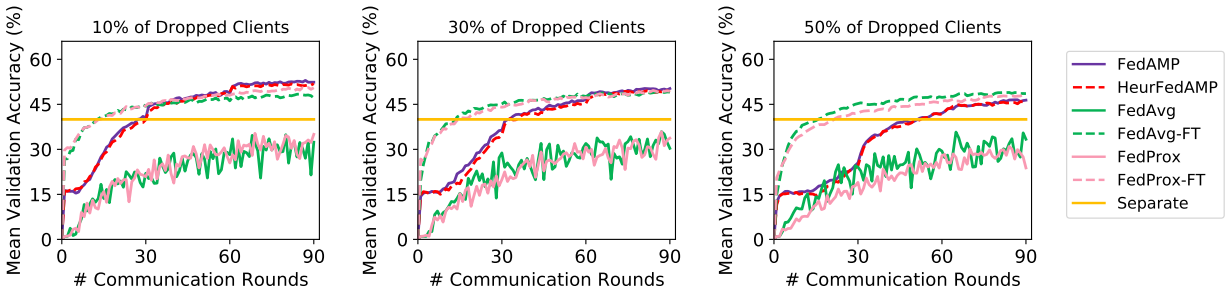


Figure 9: Performance of FEDAMP and HEURFEDAMP compared with baselines for different number of dropped clients on CIFAR100.

each client only contain 2 classes. Thus, essentially a binary classifier is trained locally. This makes the training much simpler when comparing with the IID and challenging non-IID settings, where all clients have samples from all classes.

In conclusion, the pathological non-IID data setting is not a practical non-IID data distribution for testing federated learning algorithms.

Table 6: Best mean validation accuracy for non-IID (in %)

Methods	MNIST	FMNIST	EMNIST	CIFAR100
Separate	98.73	97.67	99.15	92.67
FedAvg	98.39	77.88	19.44	2.70
FedAvg-FT	99.66	98.07	99.24	95.00
FedProx	97.15	83.80	48.81	2.81
FedProx-FT	99.63	98.00	99.27	94.36
FEDAMP	99.53	97.95	99.27	94.87
HEURFEDAMP	99.38	98.17	99.26	94.74